

# Efficiency of Ground State Quantum Computer

Wenjin Mao

Department of Physics and Astronomy, Stony Brook University, SUNY, Stony Brook, NY 11794, U.S.A.

(Dated: June 8, 2019)

The energy gap is calculated for the ground state quantum computer, which is recently proposed by Mizel et.al. We find that when implementing a quantum algorithm by Hamiltonian containing only pairwise interaction, the inverse of energy gap  $1/\Delta$  is proportional to  $N^{3k}$ , where  $N$  is the number of bits involved in the problem, and  $N^k$  is the number of control operations performed in a standard quantum paradigm. Besides suppressing decoherence due to the energy gap, in polynomial time ground state quantum computer can finish the quantum algorithms that are supposed to be implemented by standard quantum computer in polynomial time.

PACS numbers: 03.67.Lx

Quantum computer is widely believed to outperform its classical counterpart for some classically difficult problems[1, 2, 3, 4]. Although many schemes have been suggested[5, 6, 7, 8, 9, 10, 11, 12], the main obstacle is decoherence that makes very difficult the realization of even one qubit or one gate for quantum computing. Ground state quantum computer (GSQC) is a new approach proposed by Mizel et.al.[13], which replaces time evolution of a system by space distribution of ground state wavefunction. The scale of cost time for GSQC can be related with  $1/\Delta$ , with  $\Delta$  being the energy gap between the ground state and the first excited state. The advantage of GSQC is that appreciable energy gap suppresses decoherence from environment as long as temperature is lower than the energy gap, and there is no time-dependent control.

To analyze the performance of ground state quantum computer, the key issue is evaluating the scale of energy gap  $\Delta$ . However, we find calculations on energy gap by Mizel et.al.[14, 15] questionable, in which they focused on energy gap of doubly degenerated energy levels for single qubit and interacting qubits. For a GSQC to work properly it's ground state must be unique. We will show that when degeneracy is removed the energy gap is dramatically different from theirs.

In the present paper, we evaluate the energy gap  $\Delta$  of GSQC circuit in various situations, and estimate it's scale for established quantum algorithm supposed to be implemented on standard quantum computer, such as the quantum Fourier transform, the core in factorization, period finding, etc.

At first, we briefly introduce the idea of GSQC[13]. A standard computer is characterized by time dependent state as:  $|\psi(t_i)\rangle = U_i|\psi(t_{i-1})\rangle$ , where  $t_i$  denotes instance of the  $i$ -th time step, and  $U_i$  represents for unitary transformation. For GSQC, all the states in the time sequence are contained in the space distribution of the ground state wavefunction  $|\psi_0\rangle$ . The time cost is determined by the inverse of energy gap  $\Delta$ .

As proposed by Mizel et.al.[13], a single qubit may be a column of quantum dots with multiple rows, and each row contains a pair of quantum dots. State  $|0\rangle$  or  $|1\rangle$  is represented by finding electron in one of the two

dots. It is important to notice that only one electron exists in a single qubit. Other physical form of implement of GSQC may also be found. A GSQC is made up by circuit of multiple interacting qubits, whose ground state is determined by the summation of single qubit unitary transformation Hamiltonian  $h(U_j)$ , two-qubit interacting Hamiltonian  $h(CNOT)$ , boost Hamiltonian  $h(B)$  and projection Hamiltonian  $h(P)$ , as proposed by Mizel et.al[13, 14, 15].

The single qubit Hamiltonian for transformation  $U_j$  is defined as:

$$h^j(U_j) = \epsilon \left[ C_{j-1}^\dagger C_{j-1} + C_j^\dagger C_j - \left( C_j^\dagger U_j C_{j-1} + h.c. \right) \right], (1)$$

where  $C_i^\dagger = \begin{bmatrix} c_{i,0}^\dagger & c_{i,1}^\dagger \end{bmatrix}$ . The boost Hamiltonian is:

$$h^j(B, \lambda) = \epsilon \left[ C_{j-1}^\dagger C_{j-1} + \frac{1}{\lambda^2} C_j^\dagger C_j - \frac{1}{\lambda} \left( C_j^\dagger C_{j-1} + h.c. \right) \right], (2)$$

which amplifies the wavefunction amplitude by  $\lambda$  compared with previous row in the ground state. The projection Hamiltonian is

$$h^j(|\gamma\rangle, \lambda) = \epsilon \left[ c_{j-1,\gamma}^\dagger c_{j-1,\gamma} + \frac{1}{\lambda^2} c_{j,\gamma}^\dagger c_{j,\gamma} - \frac{1}{\lambda} \left( c_{j,\gamma}^\dagger c_{j-1,\gamma} + h.c. \right) \right], (3)$$

where  $|\gamma\rangle$  represents for state to be projected to. The interaction between qubit  $\alpha$  and  $\beta$  can be represented by  $h(CNOT)$ :

$$\begin{aligned} h_{\alpha,\beta}^j(CNOT) = & \epsilon C_{\alpha,j-1}^\dagger C_{\alpha,j-1} C_{\beta,j}^\dagger C_{\beta,j} \\ & + h_\alpha^j(I) C_{\beta,j-1}^\dagger C_{\beta,j-1} + c_{\alpha,j,0}^\dagger c_{\alpha,j,0} h_\beta^j(I) \\ & + c_{\alpha,j,1}^\dagger c_{\alpha,j,1} h_\beta^j(N). \end{aligned} (4)$$

where for  $c_{a,b,c}^\dagger$ , its subscription  $a$  represents for qubit  $a$ ,  $b$  for the number of row,  $c$  for the state  $|c\rangle$ . With only  $h^j(U_j)$  and  $h_{\alpha,\beta}^j(CNOT)$ , it's ground state is[14]:

$$\begin{aligned} |\psi^j\rangle = & \left[ 1 + c_{\alpha,j,0}^\dagger c_{\alpha,j-1,0} \left( 1 + C_{\beta,j}^\dagger C_{\beta,j-1} \right) \right. \\ & \left. + c_{\alpha,j,1}^\dagger c_{\alpha,j-1,1} \left( 1 + C_{\beta,j}^\dagger N C_{\beta,j-1} \right) \right] \\ & \times \prod_{a \neq \alpha, \beta} \left( 1 + C_{a,j}^\dagger U_{a,j} C_{a,j-1} \right) |\psi^{j-1}\rangle. \end{aligned} (5)$$

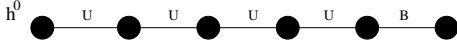


FIG. 1: A quantum dot array for single qubit. Each black dot represents for a pair of quantum dot. Label  $U$  represent for unitary transformation described by  $H(U)$ ,  $B$  for boost Hamiltonian  $H(B, \lambda)$ .

All above mentioned Hamiltonians are positive semidefinite, and are the same as those in [13, 14, 15]. Only pairwise interaction is considered for Hamiltonians involving multiple qubits.

The input states are implemented by the boundary conditions applied upon the first rows of all qubits, which can be Hamiltonian  $h^0 = E(I + \sum_i c_i \sigma_i)$  with  $\sigma_i$  being Pauli matrix and  $\sum_i c_i^2 = 1$ . For example, if  $h^0 = E(I + \sigma_z)$ , then the ground state wavefunction on the first row is  $|1\rangle$ ; if  $h^0 = E(I - \sigma_x)$ , then the state is  $(|0\rangle + |1\rangle)/\sqrt{2}$ . Unlike in [15], we set  $E \gg \epsilon > 0$ , thus boundary Hamiltonians are not perturbation. If  $E$  is large enough, the energy gap is independent of its magnitude.

Although one can analytically obtain energy gap for single qubit with  $n$  rows[14], it's difficult to calculate for a complicated circuit. However, we still manage to find its scale.

Now let's consider the simplest case: a  $n$ -row single qubit without projection or boost Hamiltonian. The Hamiltonian  $\sum_{i=1}^n h(U_i)$  is in fact the kinetic energy just like a particle in a one-dimension box with length  $n$ , thus the energy gap between the ground state and the first excited state is  $\Delta \propto \epsilon/n^2$ . Without boundary Hamiltonian, all energy levels are doubly degenerated, and in every degenerated pair, one state is orthogonal to the other on every row.

With boundary Hamiltonian  $h^0$ , the degeneracy is removed. The unique ground state  $|\psi_0\rangle$  is still uniform over all rows, and the first excited state  $|\psi_1\rangle$  is orthogonal to  $|\psi_0\rangle$  on each row. Due to large value of  $E$  in  $h^0$ ,  $|\psi_1\rangle$  on the first row is almost zero, and it is an mono-increasing function that reaches maximum on the final row, just like half of the first excited state when  $h^0 = 0$ . Thus with  $h^0 \neq 0$ , we have  $\Delta \propto \epsilon/(2n)^2$ . At ground state the probability of finding electron on any row is  $1/n$ .

As shown in Fig.(1), when a boost Hamiltonian  $h(B, \lambda)$  is applied to the qubit's final row, where the amplitude of both  $|\psi_0\rangle$  and  $|\psi_1\rangle$  are about  $\lambda$  times that at other rows, hence the wavefunction amplitude on other rows is  $O(1/\sqrt{\lambda^2 + n - 1})$ . When the electron stays at rows other than the final row, it behaves like the length of the qubit is  $\lambda + n - 1$  instead of  $n$ , and the local kinetic energy should give the correct eigenstate energy, hence if  $\lambda \gg n$  we have energy gap

$$\Delta \propto \frac{\epsilon}{(\lambda + n - 1)^2} \approx \frac{\epsilon}{\lambda^2}. \quad (6)$$

In other words, in the presence of boost Hamiltonian on the final row of a qubit, there is a parameter, the ratio of

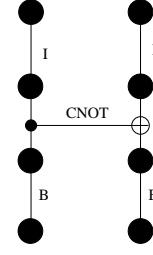


FIG. 2: Two qubits interact with each other by  $h(CNOT)$ . The label  $I$  stands for identity transformation. The left qubit is the control qubit, and the right one is the target qubit.

the lowest excited state wavefunction  $|\psi_e\rangle$  on the second row over the last row,

$$\frac{1}{x} = \frac{\langle \mathbf{R}_2 | \psi_e \rangle}{\langle \mathbf{R}_n | \psi_e \rangle}, \quad (7)$$

giving the scale of energy gap

$$\Delta \propto \frac{\epsilon}{x^2} \quad (8)$$

as long as  $x \gg n$ . The above relations Eq.(7) and Eq.(8) can be applied to multiple interacting qubits for energy gap scale estimation if all qubits are short,  $n$  is small, and  $h(B, \lambda)$  only happens on final row of each qubit with  $\lambda \gg n$ .

In [14]  $\Delta$  for a single qubit is found independent of  $\lambda$  because they first found the gap between doubly degenerated levels, and then obtained the real gap by perturbation theory, which might be right for small  $\lambda$ . However, for large  $\lambda \gg n$  perturbation theory doesn't work at all, and this also happens to their energy gap calculation for multiple qubits[14, 15].

If instead of boost Hamiltonian, a projection Hamiltonian  $h(|\gamma\rangle, \lambda)$  is applied on the last row of a single qubit, then  $|\psi_0\rangle$  on the final row is restricted to state  $|\gamma\rangle$ . Assuming besides amplitude and phase the ground state wavefunction on the second last row is at state  $|\xi\rangle$ , which is normalized, and  $\langle \xi | \gamma \rangle$  is appreciable, the ground state wavefunction will concentrate on the final row, and the first excited state wavefunction  $|\psi_1\rangle$  should have little weight there, otherwise  $\langle \psi_1 | \psi_0 \rangle \neq 0$ . Thus the energy gap  $\Delta$  remains at about  $\epsilon/n^2$ , independent of  $\lambda$ .

Numerical calculations on single qubit in various situations have confirmed all the above analysis. For example, the energy gap of a 6-row qubit ended with  $h(B, \lambda)$ , as in Fig.(1) with  $h^0 = E(I - \sigma_z)$  and  $E = 10^4 \epsilon$ , is  $\Delta = 0.08101, 0.01778, 1.976 \times 10^{-3}, 1.998 \times 10^{-4}, 2.0 \times 10^{-5} \epsilon$  at  $\lambda = 1, \sqrt{10}, 10, \sqrt{1000}, 100$  respectively, noting that the value of  $E$  is not important, and one can simply remove one of quantum dot in the first row.

Next we consider two qubits interacting with each other through  $h(CNOT)$  as shown in Fig.(2), with the left qubit as control qubit, the right one as target qubit, and both ended with  $h(B, \lambda)$ . By observing ground state

wavefunction Eq.(5), it's easy to see that it has the form

$$\begin{aligned} &(|\psi_{control}^{upstream} + |\psi_{control}^{downstream}\rangle)|\psi_{target}^{upstream}\rangle \\ &+ |\psi_{control}^{downstream}\rangle|\psi_{target}^{downstream}\rangle. \end{aligned} \quad (9)$$

The boost Hamiltonian on the final row of the target qubit raises the amplitude of  $|\psi_0\rangle$  on the downstream rows of the control qubit, while boost Hamiltonian on control qubit doesn't influence much the amplitude on the target qubit because both parts of states entangle with the downstream state of control qubit. While at ground state all kinetic energy is zero, with proper Hamiltonians the lowest excited states should not differ much from ground state concerning on weight of wavefunction distribution and kinetic energy comes from only one qubit. Thus we expect that at the first excited state  $|\psi_1\rangle$  the parameter in Eq.(7) on the control qubit is  $1/x \approx 1/\lambda^2$ . The second excited state  $|\psi_2\rangle$  on the target qubit has  $1/x \approx 1/\lambda$ .

Numerical calculation shows that,  $|\psi_1\rangle$  on the first two rows of control qubit is orthonormal to ground state, while states on the first two rows of target qubit is the same as ground state, and  $1/x \approx 1/\lambda^2$ , the eigenenergy is from the kinetic energy of the control qubit, and  $\Delta = E_1 \propto \epsilon/\lambda^4$ , agreeing with Eq.(8). The states of  $|\psi_2\rangle$  on the first two rows of target qubit are orthonormal to ground state, while states on the first two rows of control qubit are the same as ground state. However, we find that  $1/x$  in  $|\psi_2\rangle$  on the target qubit is still  $1/x \approx 1/\lambda^2$ , and the eigenenergy is  $E_2 \propto \epsilon/\lambda^4$ , different from our expectation that this state should have  $1/x \approx 1/\lambda$ . This is because the second excited state has different form from  $|\psi_0\rangle$  concerning on wavefunction distribution. We modify the definition of  $h(CNOT)$  as:

$$\begin{aligned} h_{\alpha,\beta}^j(CNOT') &= \epsilon C_{\alpha,j-1}^\dagger C_{\alpha,j-1} C_{\beta,j}^\dagger C_{\beta,j} \\ &+ h_{\alpha}^j(I) C_{\beta,j-1}^\dagger C_{\beta,j-1} + \sum_{i=j}^n c_{\alpha,i,0}^\dagger c_{\alpha,i,0} h_{\beta}^j(I) \\ &+ \sum_{i=j}^n c_{\alpha,i,1}^\dagger c_{\alpha,i,1} h_{\beta}^j(N). \end{aligned} \quad (10)$$

By the new  $h(CNOT')$ , the transfer term is enhanced between upstream and downstream on target qubit, and now in the second excited state the wavefunction distribution is similar with  $|\psi_0\rangle$ , and  $1/x \approx 1/\lambda$  on the target qubit and  $E_2 \propto \epsilon/\lambda^2$ . However, the implement of  $h(CNOT')$  requires the downstream part of target state doesn't experience any transformation, thus it cannot be used everywhere.

If projection Hamiltonians are applied instead of boost Hamiltonians, and at the ground state  $\langle \xi | \gamma \rangle$  is appreciable, where  $|\xi\rangle$  is the state on the row before projection Hamiltonian at ground state, then  $\Delta \propto \epsilon/\lambda^2$  due to the same reason as for single qubit. It is interesting to note that by projecting the target qubit into one state on its last row and boost this state, one can manipulate the

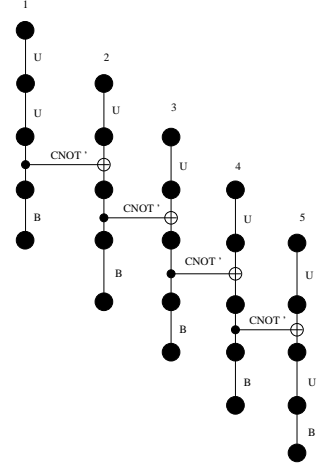


FIG. 3: A chain of qubits interact with each other through  $H(CNOT')$ . Note that except for the two qubits on the ends, each qubit interacts as both control qubit and target qubit and the control directions are the same. This is the circuit with the smallest energy gap.

state on the final row of the control qubit, and this can be observed in Eq.(9).

Numerical calculations confirm our analysis. For example, the energy gap for two 4-row qubits ended with  $h(B, \lambda)$ , as shown in Fig.(2) with  $h_1^0 = E(I - \sigma_x)$ ,  $h_2^0 = E(I + \sigma_z)$  and  $E = 10^4\epsilon$ , is  $\Delta = 0.06095, 3.198 \times 10^{-3}, 4.492 \times 10^{-5}, 4.677 \times 10^{-7}, 4.696 \times 10^{-9}\epsilon$  at  $\lambda = 1, \sqrt{10}, 10, \sqrt{1000}, 100$  respectively.

With multiple qubits interacting with each other, just like the two qubits case, the lowest excited state has similar distribution with  $|\psi_0\rangle$  and on only one qubit's first two rows the states are orthonormal to  $|\psi_0\rangle$  while states on other qubits contribute nearly zero energy. We need to evaluate on each qubit the ratio  $1/x$  defined in Eq.(7), then the minimum  $1/x$ , which usually happens on a qubit acting as control qubit, gives roughly the energy gap as  $\epsilon/x^2$ . Thus the energy gap depends on the detail of the circuit.

For example, in Fig.(3) qubit 1  $CNOT$  controls qubit 2, and in the downstream part, qubit 2  $CNOT$  controls qubit 3, so on to qubit 5. When all qubits end with a boost Hamiltonian  $H(B, \lambda)$ , we find that, for  $\lambda \gg 5$ , the parameter in Eq.(7) is  $x = \lambda$  for qubit 5 at the right side,  $x = \lambda^2$  for qubit 4,  $x = \lambda^3$  for qubit 3, and for qubit 1,  $x = \lambda^5$ . Thus the energy gap of the circuit is determined by the minimum value of  $1/x$ , which is on the first qubit, hence  $\Delta \propto \epsilon/\lambda^{10}$ . If any one of the  $h(CNOT)$  switches direction of control, the energy gap will increase. The circuit in Fig.(3) is one with least energy gap. There is another circuit that also has the least scale of energy gap, such as one qubit  $CNOT$  controlling many other qubits with all qubits ended with boost Hamiltonian.

We conclude that the energy gap of a ground state quantum computer may be exponentially small depending on detail of problems.

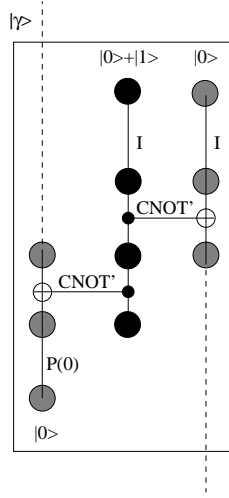


FIG. 4: Circuit for transfer box with label  $P(0)$  representing for projection Hamiltonian  $h(|0\rangle, \lambda)$ . The input qubit state on the left is  $|\gamma\rangle = a|0\rangle + b|1\rangle$ , and the output state of the two qubits on right side is  $a|0\rangle|0\rangle + b|1\rangle|1\rangle$  with large probability, hence the quantum state at the left qubit is transferred to the right qubit.

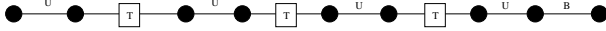


FIG. 5: A single qubit experiences  $N$  unitary transformations, and transfer boxes are inserted between each transformation. For this circuit the energy gap  $\Delta$  is proportional to  $1/N^2$ .

Fig.(7) in [15] shows how to use teleport technique[16] to increase  $\Delta$ , however, their energy gap estimation is not correct due to the reason mentioned above, and we estimate  $\Delta \propto 1/N^3$ . Here we introduce a simpler way to transfer quantum information, the transfer box shown in Fig.(4), where  $h(CNOT')$  is used instead of  $h(CNOT)$ . It's not difficult to find that if input state is  $|\gamma\rangle = a|0\rangle + b|1\rangle$  and if all three electrons are found at the lowest rows in the box, then the state is  $|0\rangle(a|0\rangle|0\rangle + b|1\rangle|1\rangle)$ , thus quantum information on the left qubit is transferred to the qubit on the right side. If we insert the transfer box between each of the  $N$  unitary transformations happened on a single qubit, it is found that the energy gap is  $\Delta \propto 1/\lambda^4$  because the lowest value of  $1/x \approx 1/\lambda^2$  on the middle qubit in the transfer box, where each of the two qubits next to it contributes a  $\lambda$ . The probability to measure correct result in the final row of the last qubit is  $P \approx (1 - C/\lambda^2)^N$  with  $C$  being of order 1, thus we have to set  $\lambda = \sqrt{N}$  in order to make  $P$  independent of  $N$ . It appears that for single qubit case the energy gap doesn't change, still is of the order  $O(1/N^2)$ . However, for a single qubit, there is no need to implement multiple unitary transformations, one can always combine them into one transformation and implement it by GSQC.

Now we can check the energy gap when a quantum

algorithm is implemented by GSQC. The most powerful quantum algorithm up to now is quantum Fourier transform, which is used in factorization, period finding, etc. The detail of quantum Fourier transform, more precisely, the inverse quantum Fourier transform, can be found in many literatures, such as [17]. It takes  $O(N^2)$  control operations  $h(CR_k)$  to carry out inverse quantum Fourier transform by standard time dependent approach, where  $N$  is the number of qubits involved in the problem, and  $R_k$  is the unitary transformation shifting phase of state  $|1\rangle$  by  $2\pi i/2^k$ [17].  $h(CR_k)$  can be obtained by replacing  $NOT$  operator by  $R_k$  in Eq.(5). One can simply replace the time evolution by circuit array and calculate the energy gap of the circuit. In order to increase the energy gap, and also increase the probability of finding electrons in the final rows of qubits in GSQC, two transfer boxes are inserted after each control Hamiltonian so that the two qubit's quantum states are transferred to new qubits and calculation is continued on the new qubits. In the end, all qubits ended with the same boost Hamiltonian  $h(B, \lambda)$ . The middle qubit in the transfer box, Fig.(4), interacts with the two qubits besides it as control qubit, thus the chain like in Fig.(3) doesn't exist, and the energy gap will not be exponentially small.

According to Eq.(7) and Eq.(8), the energy gap is not difficult to find: the parameter  $1/x$  on the middle of every transfer box is the least, where  $1/x \approx 1/\lambda^3$ , with a  $\lambda$  from the left side qubit, and  $\lambda^2$  from the right hand qubit because that qubit will experience a  $h(CR_k)$  as control qubit with a qubit downstream, and both of them ended with projection Hamiltonian. There are totally  $O(N^2)$   $h(CR_k)$  to be implemented, hence in order to make the probability  $P \approx (1 - C/\lambda^2)^{KN^2}$  be finite with  $K$  being of order 1, one has to set  $\lambda \approx O(N)$ , thus we obtain  $\Delta \approx 1/x^2 \approx O(1/N^6)$ , noting that standard paradigm needs only  $N^2$  steps.

Time needed by ground state quantum computer is determined by the number of control operation. We conclude that any quantum algorithm implemented by standard paradigm can be implemented by GSQC, and the energy gap is  $\Delta \propto 1/N^{3k}$ , where  $N$  is the number of bits in the problem, and  $N^k$  is the number of control operations needed in standard quantum paradigm.

Quantum algorithms implemented by standard paradigm in polynomial time may be implemented by ground state quantum computer in polynomial time, and the energy gap may suppress environment decoherence, hence GSQC might be more feasible than other forms of quantum computer. On the other hand, while it doesn't make sense to implement Grover's algorithm by GSQC like we presented in this paper, there are some algorithms that standard paradigm cannot realize while GSQC might enable, and we will report those algorithms in following work.

I would like to thank A. Mizel for discussion. This work was supported in part by the NSF under grant # 0121428 and by ARDA and DOD under the DURINT grant # F49620-01-1-0439.

- 
- [1] P. Shor, in *Proceedings of the 35th Annual Symposium on the Foundations of Computer Science, Los Alamitos, California, 1994*, edited by Goldwasser (IEEE Computer Society Press, New York, 1994), p. 124.
  - [2] L.K. Grover, *Phys. Rev. Lett.* **79**, 325(1997).
  - [3] E. Farhi, J. Goldstone, S. Gutmann, J. Lapan, A. Lundgren, D. Preda, *Science*, **292**, 472(2001).
  - [4] J. Roland and N.J. Cerf, *Phys. Rev. A* **65**, 042308(2002).
  - [5] Q. A. Turchette *et al.* *Phys. Rev. Lett.* **75**, 4710 (1995).
  - [6] I. L. Chuang, N. Gershenfeld, M. Kubinec, *Phys. Rev. Lett.* **80**, 3408 (1998).
  - [7] D. Loss and D. P. DiVincenzo, *Phys. Rev. A* **57**, 120 (1998).
  - [8] G. Burkhard, D. Loss, D. P. DiVincenzo, *Phys. Rev. B* **59**, 2070 (1999).
  - [9] Y. Makhlin, G. Schon, A. Shnirman, *Nature* **398**, 305 (1999).
  - [10] D. V. Averin, *Solid State Commun.* **105**, 659 (1998).
  - [11] B. Kane, *Nature* **393**, 133 (1998).
  - [12] L. B. Ioffe, V. B. Geshkenbein, M. V. Feigel'man, A. L. Fauchere, G. Blatter, *Nature* **398**, 679 (1999).
  - [13] A. Mizel, M.W. Mitchell and M.L. Cohen, *Phys. Rev. A*, **63**, 040302(2001).
  - [14] A. Mizel, M.W. Mitchell and M.L. Cohen, *Phys. Rev. A*, **65**, 022315(2002).
  - [15] A. Mizel, *Phys. Rev. A*, **70**, 012304(2004).
  - [16] M.A. Nielsen and I.L. Chuang, *Phys. Rev. Lett.* **79**, 321(1997).
  - [17] M.A. Nielsen and I.L. Chuang, *Quantum Computation and Quantum Information*, Cambridge University Press, 2000.